Synthesis, Characterization, and Theoretical Calculation of New Azo Dyes Derived from [1,5-*a*]Pyrimidine-5-one Having Solvatochromic Properties

Nesrin Şener,[a]* ID Mahmut Gür,[b] ID M. Serdar Çavuş,[c] ID Merve Zurnaci,[d] and İzzet Şener[e] ID

[a]Department of Chemistry, Faculty of Science-Arts, Kastamonu University, 37200 Kastamonu, Turkey
[b]Department of Forest Industrial Engineering, Faculty of Forestry, Kastamonu University, 37200 Kastamonu, Turkey
[c]Department of Biomedical Engineering, Faculty of Engineering and Architecture, Kastamonu University, 37200 Kastamonu, Turkey
[d]Institute of Science, Kastamonu University, 37200 Kastamonu, Turkey
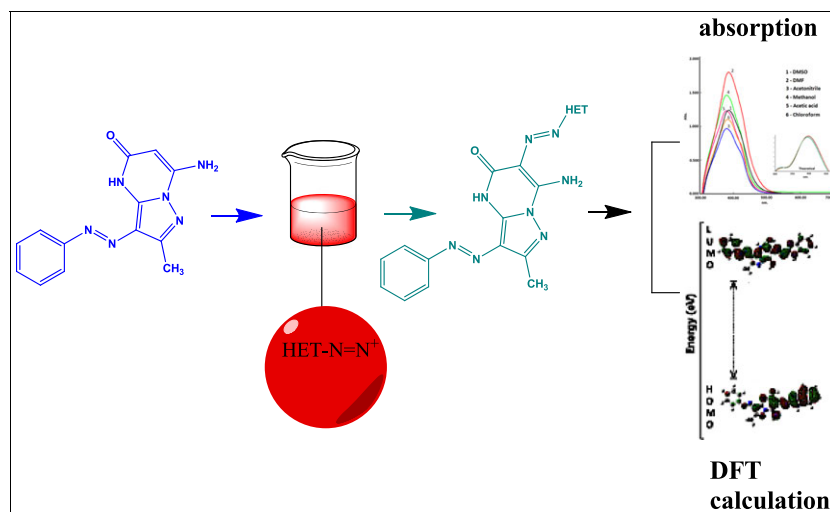[e]Department of Food Engineering, Faculty of Engineering and Architecture, Kastamonu University, 37200 Kastamonu, Turkey
*E-mail: nsener@kastamonu.edu.tr

7-Amino-3-phenylazo-2-methyl-4*H*-pyrazolo[1,5-*a*]pyrimidine-5-one (**3**) was synthesized by the reaction of 5-amino-3-methyl-4-phenylazo-1*H*-pyrazole and 2-aminobenzothiazole with ethyl cyanoacetate in acetic acid at 150°C. Four novel heterocyclic azo disperse dyes were obtained by the coupling of heterocyclic amines-based diazonium chloride with compound **3**. They were purified and characterized by elemental analysis, FTIR, and ^{1}H NMR. Furthermore, solvatochromic behaviors of related dyes were studied in detail by using ultraviolet–visible absorption spectrometer. The experimental data were supported by density functional theory using b3lyp/cc-pvtz level calculations, and a detailed analysis of predicted tautomeric structures was made.

INTRODUCTION

Azo dyes are well-known compounds for giving color to various textile materials for many years [1–4]. These dyes play also a major role in industrial products such as printing, leather, papermaking, food industries, and drug design, except for textile dyeing [5,6]. Besides, they are manufactured in technological purposes for multiple optical and electronic applications such as second harmonic generation, optical switching, chemosensing, and organic-sensitized solar cells [7,8]. It has been known that conjugation of suitable heterocyclic moiety such as thiophene, pyrrole, and azoles with azo compounds enhance some properties such as biological activity [9,10], dyeing fastness [11–13], and electronic properties [14]. Azo dyes bearing heterocyclic moiety are widely synthesized, and it has been reported that they have better tinctorial strength and brighter dyeing than aniline-based dyes [15]. For example, in a study of Hallas *et al.*, after azo dyes were synthesized by reaction of 2-aminothiophene derivatives and various heterocyclic coupling components, it was applied on polyester fibers [16]. It was reported that *N*-containing and/or *S*-containing heterocyclic azo dyes such as thiophene, thiazole, thiadiazole, benzothiazole, and benzoisothiazole have shown many benefits in the aspects of brightness, fastness, color-deepening, and brilliant dyeing properties than azo dyes derived from azobenzene, in recent years [17,18]. Furthermore, many studies on tautomerism of azo dyes are also available in the literature, and their tautomerism is related with some fields such as optical, technical, and environmental applications [19,20]. The

tautomeric equilibrium primarily depends on structural factors, solvent polarity, and pH of the medium. Also, some researchers have investigated the tautomerism of azo dyes using density functional theory (DFT) calculations [21].

Additionally, the dyes bearing pyrazolo[1,5-a] pyrimidine and its derivatives are also used as intermediates in the dyestuff industry although they are known to possess many biological activities [22,23].

Biologically active molecules can be obtained by increasing the number of functional groups on azo compounds including heteroaromatic structures [24]. The 5-aminopyrazoles bound to create a biological effect on the structure of many compounds are versatile reagents and have been extensively used as synthetic starting components for the preparation of many polyfunctional compounds [25]. Pyrazoles derivatives that are important heterocyclic classes have very versatile biological properties such as antihyperglycemic [26], analgesic [27], anti-inflammatory [28], antipyretic [29], antibacterial [30], and hypoglycemic activity [31,32].

The reaction of heterocyclic aromatic amines with coupling compounds by diazotization in both anhydrous and aqueous media has been tried by a number of researchers. In this work, four different heterocyclic azo dyes with different aromatic amines were synthesized. Synthesis methods of the compounds were described in detail at our previous work [33]. Moreover, FTIR, ultraviolet–visible (UV–Vis), and ^{1}H NMR spectra of the compounds were performed by using the B3LYP method with cc-pvtz basis set. The highest occupied molecular orbital (HOMO), lowest unoccupied molecular orbital (LUMO) energies, and some parameters such as electronegativity, chemical hardness, and polarizability (α) were also calculated using the same method and basis set. The relationship between tautomeric forms and electronic properties of the compounds was theoretically investigated. Furthermore, the keto forms and possible tautomeric structures of the compounds were investigated to see how the tautomeric forms affected the structural and spectral properties of the compounds.

It is well known that the color of halochromic molecules changes depending on the pH, so that reversible changes are observed in the colors of the materials at certain pH intervals, depending on the halochromism. The propensity of halochromic behavior is significantly affected from the electronic situation of substituents such as electron-withdrawing and electron-donating. The difference between the absorption maxima of protonated and deprotonated molecules arises from these effects of substituents. Based upon this view, it can be said that dyes have equilibrium of tautomeric forms (azo/hydrazo), and the azo form predominates in basic media although the hydrazo form is dominated in the acidic media [34]. Therefore, in this study, how absorption is changed in acidic, and basic environment is also examined.

RESULTS AND DISCUSSION

Calculated electronic parameters such as minimum molecular energy (E), HOMO-LUMO energy gap (ΔE), chemical hardness (η), electronegativity (χ), polarizability (α), and dipole moment (μ) are given in Table 1. The ability of an examined molecule to interact with the surrounding environment is proportional to the total dipole moment. The dipole moment of compound **4d** (7.73 Debye) was calculated to be about 1.5-2 times greater than other compounds; this indicates a higher reactivity to interact with the environment surrounding it. ΔE is useful to characterize the chemical reactivity and kinetic stability of a molecule. The HOMO-LUMO energy gap of compound **4c** was calculated to be lower, indicating that its chemical reactivity is higher than other compounds. The HOMO-LUMO surfaces of the compounds are given in Figure 1. While the LUMO energies of the compounds were more stable, compound **4c** had the highest HOMO energy, which means that it exhibits greater anti-bonding behavior. Moreover, the polarizability of compound **4d** was calculated as the lowest, but ΔE to be the highest.

Ultraviolet–visible analysis of the compounds. Ultraviolet–visible absorption spectra were recorded on a Shimadzu (Japan) UV-1601 UV–vis spectrophotometer over the λ range of 300 to 700 nm, using a variety of solvents in a solution concentration of 1×10^{-5} M.

Table 1

Calculated electronic parameters of the compound **4(a–d)**.

Comp.	E (au)	E_{HOMO} (eV)	E_{LUMO} (eV)	ΔE (eV)	η (eV)	χ (eV)	α (au)	μ Debye
Pri.	−906.64	−6.04	−2.21	3.84	1.92	4.13	232.67	3.91
4a	−1394.91	−5.82	−2.70	3.12	1.56	4.26	438.38	3.32
4b	−1737.75	−6.03	−2.83	3.20	1.60	4.43	447.22	4.62
4c	−1852.31	−5.71	−2.74	2.97	1.48	4.23	485.79	4.99
4d	−1300.36	−6.19	−2.64	3.55	1.77	4.41	353.55	7.73

Pri., primidone ring; E, energy; ΔE, $E_{LUMO} - E_{HOMO}$; η, chemical hardness; χ, electronegativity; α, polarizability; μ, dipole moment.
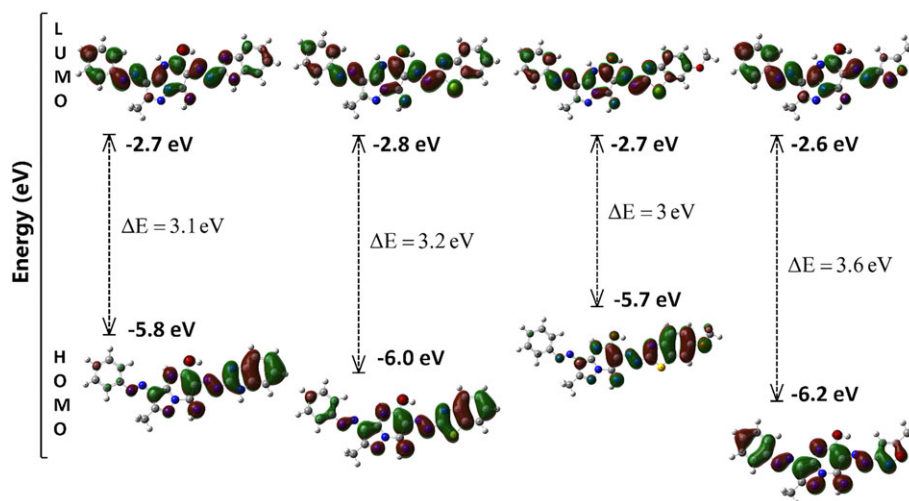
Figure 1. Highest occupied molecular orbital–lowest unoccupied molecular orbital (HOMO-LUMO) surfaces/energy gab of compound **4(a–d)**, respectively. [Color figure can be viewed at wileyonlinelibrary.com]

The absorption maxima of the dyes are tabulated in Table 2.

It can be seen that the compounds give the single maximum absorption point. It can be argued that the shoulder-free structures in the UV spectra are in a single tautomeric form in these solvents; in other words, the maximum absorption points of the compounds do not vary much with respect to the solvents. However, at the absorption values of dyes were observed a hypsochromic shift other solvents than *N,N*-dimethylformamide (DMF) and dimethyl sulfoxide (DMSO). Based on this observation, it can be said that absorption wavelengths increase with increasing dielectric constants of the solvent. For example, for the dye **4d**, λ_{max} values are 386 nm in DMSO, 385 nm in DMF, 380 nm in acetonitrile, 379 nm in methanol, and 379 nm in acetic acid (Fig. 2).

Experimental observations were also supported by theoretical UV calculations. The absorption spectra for six predicted tautomers of the compound **4(a–d)**, which was calculated in the acetic acid, are given in Figure 3. Based on theoretical calculations, it was seen that the pyrimidone ring and the heterocyclic ring are not on the same plane for tautomers T1, T3, and T4 (the first group) but are on the same plane for tautomers T2, T5, and T6 (the second group) (Scheme 3). In addition, the minimum
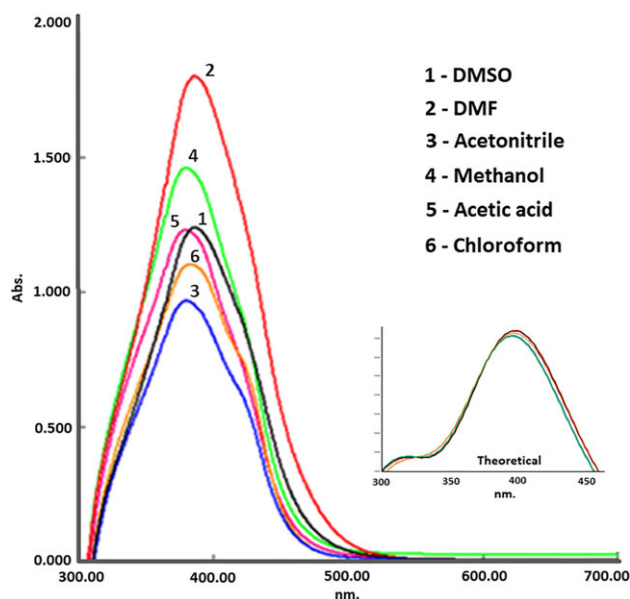

Figure 2. Experimental and theoretical absorption spectra of dye **4d** in various solvents. [Color figure can be viewed at wileyonlinelibrary.com]

molecular energies of the second group of tautomers (between 1394.11 and 1394.88 au) were calculated to be lower than that of the first group (between 1394.92 and

Table 2

Absorption data of the dyes in different solvents (nm).

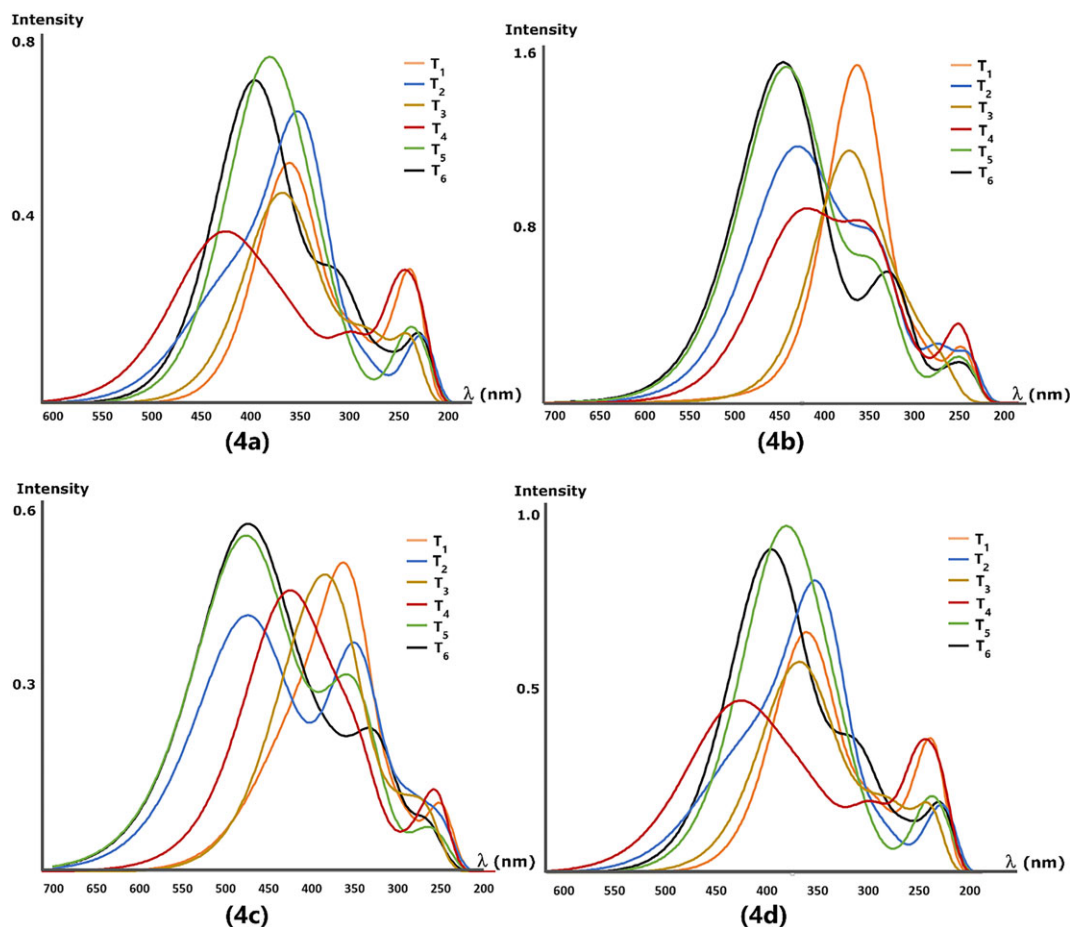| Compound no.	DMSO	DMF	Acetonitrile	Methanol	Acetic acid	Chloroform
4a	372	374	364	363	363	365
4b	372	373	365	362	363	366
4c	371	375	364	363	362	364
4d	386	385	380	379	379	384

Figure 3. The ultraviolet absorption maxima of the compounds calculated in the acetic acid. [Color figure can be viewed at wileyonlinelibrary.com]

1394.96 au), indicating that the second group of tautomeric structures is more likely to be obtained experimentally. For the first group, because of the higher electron density in the pyrimidone ring, the moving of the hydrogen atom of the pyrimidone ring to the nitrogen of the azo group bound to the phenyl ring *via* electron transfer has a lower probability. Therefore, the probability of occurrence of the tautomer T_4 is less than the others. In addition, theoretical UV calculations were not consistent with experimental results for tautomer T_4 (Fig. 3).

The calculated UV data of the six possible tautomers of the synthesized compounds in six different solvents are given in Table 3. Because the UV calculations are directly related to the HOMO-LUMO energy gab ΔE, which is particularly affected by the conformational structure, it is difficult to obtain enough information about the tautomer structure by looking only at the UV absorption peaks.

The formation of tautomeric structures in a synthesis process is directly related to environmental factors such as pressure and temperature, as well as to a number of parameters such as solvent effect and impurity. Besides,

it is well known that any molecular structure attempt to reach the lowest energy. Furthermore, the thermodynamic stability of a state of matter is not only dependent on the energy difference between the states. Also, the lower the electronegativity of a molecule, the weaker it tends to bond with the electrons of the environment atoms (or molecules). In addition to being dependent on many factors including temperature, solvent, and pH, the ratio of tautomers should be proportional to the electronegativity of a molecule. For each compound, it was observed that the electronegativity of the tautomer T_6 was lower than those of the others. Electronegativity values of the tautomer of compound **4(a–d)** calculated in DMF are given in Figure 4. Tautomer T_6 is more likely to be theoretically than the other tautomeric structures; this situation was also detailed by analyzing ^{1}H NMR data in the section ^{1}H NMR analysis of the compounds.

We also observed how the absorption graphs of compounds changed with methanol and with the addition of both HCl and KOH to methanol, and these results are given in Table 4.

Table 3
Calculated ultraviolet–visible absorption maxima of tautomer structures of compound **4(a–d)**.

		Acetic acid		Acetonitrile		DMF		DMSO		Chloroform		Methanol	
		$\lambda_{max,\,1}$	$\lambda_{max,\,2}$	$\lambda_{max,\,1}$	$\lambda_{max,\,2}$	$\lambda_{max,\,1}$	$\lambda_{max,\,2}$	$\lambda_{max,\,1}$	$\lambda_{max,\,2}$	$\lambda_{max,\,1}$	$\lambda_{max,\,2}$	$\lambda_{max,\,1}$	$\lambda_{max,\,2}$
4a	T_1	365	-	365	-	367	-	367	-	366	-	365	-
	T_2	445	345	445	344	447	345	447	345	447	347	445	344
	T_3	383	-	381	-	382	-	382	-	385	-	381	-
	T_4	446 (s)	347	445 (s)	348	447 (s)	349	447 (s)	349	448 (s)	347	445 (s)	347
	T_5	447	347	445	346	448	348	447	347	449	349	445	346
	T_6	449	324 (s)	447	324 (s)	450	324 (s)	449	324 (s)	451	324 (s)	446	324 (s)
4b	T_1	365	-	365	-	367	-	364	-	366	-	365	-
	T_2	445	348 (s)	446	347 (s)	448	349 (s)	448	349 (s)	445	391 (s)	446	347 (s)
	T_3	383	-	381	-	382	-	382	-	384	-	381	-
	T_4	433	345 (s)	431	347 (s)	434	348 (s)	433	348 (s)	436	345 (s)	431	347 (s)
	T_5	445	346 (s)	446	344 (s)	449	345 (s)	449	345 (s)	447	347 (s)	446	344 (s)
	T_6	451	327	447	327	450	328	449	328	451	328	446	327
4c	T_1	366	-	367	-	368	-	368	-	367	-	367	-
	T_2	478	347	479	347	481	348	481	348	479	349	479	346
	T_3	421	379	425	377	429	378	430	378	420	381	425	377
	T_4	434	-	433	-	435	-	435	-	437	-	433	-
	T_5	480	349 (s)	480	348 (s)	483	349 (s)	482	349 (s)	482	350 (s)	480	348 (s)
	T_6	479	331 (s)	479	330 (s)	482	331 (s)	481	331 (s)	481	331 (s)	478	330 (s)
4d	T_1	362	298	361	298	363	299	363	299	363	298	361	298
	T_2	427	353	426	353	427	354	426	354	428	354	425	353
	T_3	378	-	371	-	373	-	373	-	379	-	371	-
	T_4	436	-	435	-	437	-	437	-	438	-	434	-
	T_5	396	-	398	-	400	-	400	-	397	-	398	-
	T_6	398	313 (s)	398	313 (s)	399	313 (s)	399	313 (s)	400	314 (s)	397	312 (s)

DMF, *N,N*-dimethylformamide; DMSO, dimethyl sulfoxide; s, shoulder.
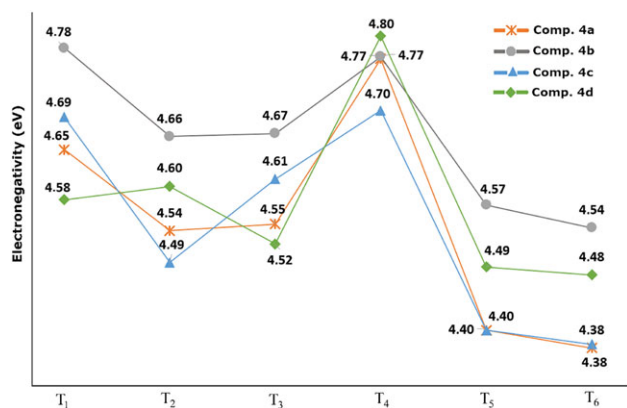

Figure 4. Electronegativity values of the tautomer of compound **4(a–d)** calculated in *N,N*-dimethylformamide. [Color figure can be viewed at wileyonlinelibrary.com]

Table 4
Absorption data of the dyes in acidic and basic solutions (nm).

Comp.	Methanol	Methanol + HCl	Methanol + KOH
4a	363	351, 459	390, 431[s]
4b	362	354, 454	390, 431[s]
4c	363	356, 455	388, 429[s]
4d	379	379, 343[s], 465[s]	381, 442, 333[s]

s, shoulder.

When the change was examined by addition of acid and base, it was generally observed that the absorption points showed bathochromic shift. Two different maximum absorption points were observed by addition of acid in all compounds except compound **4d**. The first of these newly formed wavelengths was hyposochromic shift, and the second was bathochromic shift. For example, the maximum wavelength for compound **4a** is as follows; 363 nm (in methanol), 351 and 459 nm (in acidic solution), and 390 nm (in basic solution). Figure 5 shows the change graph by the addition of the acid–base of the compound. The increase of the wave by increasing the protonation caused by the acid addition in the structures is known as positive halochromism. Then we can say that the dyes show positive halochromism. In addition, two different shoulders are observed in short and long wavelengths of the band of compound **4d**. Addition of base to methanol showed the bathochromic shift of the maximum absorption points and two different maximum points for compound **4d**. In addition, shoulders were seen in all compounds with the addition of base. This shows that the compounds are not in a single tautomeric form in these solvents.

Fourier transform infrared spectroscopy analysis of the compounds. In the experimental and theoretical FTIR spectra of the compounds, the broad bands resulting from O—H stretching vibrations were seen in the range of
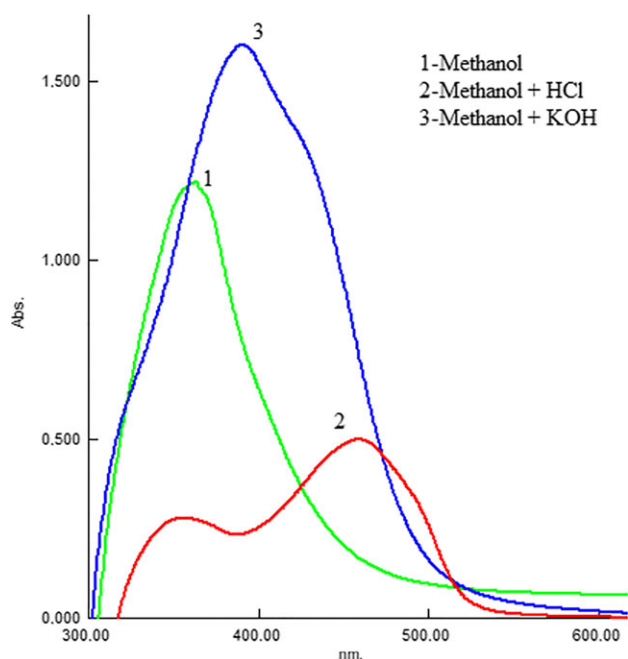
Figure 5. Absorption spectra of the dye **4a** in acidic and basic solutions. [Color figure can be viewed at wileyonlinelibrary.com]

3365–3231 cm^{-1} (theoretically 3649–3611 cm^{-1}), from N—H stretching vibrations were seen in the range of 3212–3140 cm^{-1} (theoretically 3378–3361 cm^{-1}), and

from =NH stretching vibrations were seen in the range of 3237–3170 cm^{-1} (theoretically 3468–3465 cm^{-1}). In addition, O—H stretching vibrations were seen in the range of 3212–3065 cm^{-1} (theoretically 3478–3361 cm^{-1}). While the broad peak of small intensity situated in the range 3066–3059 cm^{-1} (theoretically 3199–3188 cm^{-1}) was assigned to aromatic C—H stretching vibrations, aliphatic C—H stretching vibrations were also identified at the range of 2991–2924 cm^{-1} (theoretically 3045–3006 cm^{-1}). The bands associated to C=N bonds on the aromatic rings were seen at 1609–1557 cm^{-1} (theoretically 1717–1714 cm^{-1}). The bands at the range of 1555–1521 cm^{-1} (theoretically 1554–1525 cm^{-1}) were associated to N=N stretching vibrations. The band associated to C—S—C stretching
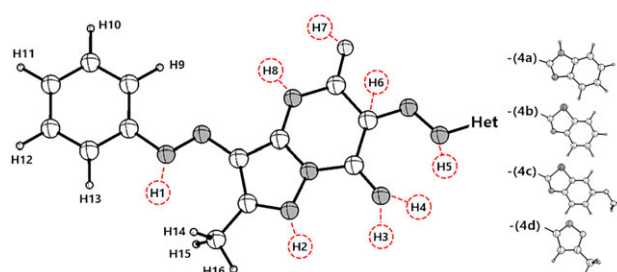

Figure 6. The general structural illustration of the predicted tautomers. [Color figure can be viewed at wileyonlinelibrary.com]

Table 5

Experimental and theoretical Fourier transform infrared spectroscopy values of the compounds (cm^{-1}).

	Com.	ν O—H	ν N—H	ν =NH	ν C—H$_{Ar}$	ν C—H$_{Aliph}$	ν C=N	ν N=N	ν C—S—C	ν C—O
Experimental	**4a**	3356	3165	3198	3065	2974	1557	1528	-	-
	4b	3231	3140	3170	3059	2951	1609	1555	710	-
	4c	3334	3212	3237	3064	2991 2924	1589	1548	706	1070
	4d	3365	3198	3235	3066	2925	1583	1528	-	-
Calculated	**4a**	3649 3613	3378	3465	3198–3188	3045	1712	1554 1532	-	-
	4b	3611	3366	3468	3199–3188	3045	1715	1532 1525	663	-
	4c	3612	3367	3467	3197–3188	3045 3006	1714	1532 1526	655	1078
	4d	3615	3361	3467	3197–3188	3045	1717	1532 1525	-	-

Table 6

^{1}H NMR (δ, ppm, in DMSO-d_6) values related to synthesized compounds.

Comp.	δ Aliphatic—H	δ Aromatic—H	δ =N—H	δ N—H	δ O—H
4a	2.62 (s, 3H —CH$_3$)	7.41–7.96 (10H)	11.18	13.02	15.98
4b	2.63 (s, 3H —CH$_3$)	7.41–7.95 (9H)	11.12	12.02	13.00
4c	2.59 (s, 3H —CH$_3$) 3.85 (s, 3H —OCH$_3$)	6.46–8.03 (8H)	10.22	10.88	12.23
4d	2.45 (3H, s, pyrazole —CH$_3$) 2.60 (s, 3H isoxazole —CH$_3$)	6.46–8.01 (6H)	9.87	10.77	12.16

Table 7
Calculated ^{1}H NMR data of the compounds and their tautomers (TMS:31.8821).

		H1	H2	H3	H4	H5	H6	H7	H8	$\delta_{Aliphatic-H}$ (Pri.)	$\delta_{Aliphatic-H}$ (Het)	$\delta_{Aromatic-H}$ (Pri.)	$\delta_{Aromatic-H}$ (Het)
4a	T$_1$	-	-	10.17	-	-	6.82	-	8.6	2.75	-	8.43–7.92	8.27–7.90
	T$_2$	-	-	9.33	-	16.78	-	-	8.8	2.78	-	8.45–7.97	8.10–7-78
	T$_3$	-	8.55	9.10	-	-	6.75	-	-	2.91	-	8.49–7.92	8.24–7-88
	T$_4$	10.57	-	9.62	-	-	6.83	-	-	2.86	-	8.37–7.64	8.23–7.87
	T$_5$	-	-	7.59	11.54	-	-	-	8.95	2.83	-	8.47–7.97	8.16–7.79
	T$_6$	-	-	9.58	-	-	-	10.98	9.34	2.83	-	8.51–7.99	8.18–7.81
4b	T$_1$	-	-	9.69	-	-	9.16	-	8.84	2.79	-	8.48–7.98	8.65–8.16
	T$_2$	-	-	10.02	-	16.79	-	-	8.84	2.78	-	8.45–7.94	8.36–7.87
	T$_3$	-	8.53	9.11	-	-	6.85	-	-	2.92	-	8.32–7.92	8.58–8.03
	T$_4$	10.64	-	9.18	-	-	5.49	-	-	2.90	-	8.49–7.72	8.62–8.08
	T$_5$	-	-	7.68	11.68	-	-	-	8.97	2.83	-	8.47–7.98	8.43–7.89
	T$_6$	-	-	9.70	-	-	-	11.023	9.42	2.83	-	8.52–7.99	8.46–7.90
4c	T$_1$	-	-	10.14	-	-	6.87	-	8.59	2.75	4.15	8.44–7.92	8.59–7.68
	T$_2$	-	-	9.96		16.76	-	-	8.81	2.77	4.12	8.45–7.97	8.28–7.50
	T$_3$	-	8.61	8.86	-	-	5.22	-	-	2.99	4.15	8.55–7.98	8.47–7.65
	T$_4$	10.58	-	8.88	-	-	8.19	-	-	2.84	4.17	8.47–7.67	8.62–7.72
	T$_5$	-	-	7.61	11.57	-	-	-	8.95	2.82	4.14	8.46–7.98	8.38–7.55
	T$_6$	-	-	9.62	-	-	-	10.954	9.37	2.83	4.14	8.52–7.97	8.40–7.55
4d	T$_1$	-	-	10.20	-	-	6.8	-	8.80	2.69	2.68	8.44–7.95	6.53
	T$_2$	-	-	8.92	-	10.12	-	-	8.76	2.74	2.68	8.44–7.94	6.74
	T$_3$	-	8.59	8.74	-	-	6.04	-	-	2.98	2.76	8.57–7.98	6.04
	T$_4$	10.68	-	9.42	-	-	5.25	-	-	2.91	2.66	8.50–7.72	6.39
	T$_5$	-	-	7.51	11.63	-	-	-	8.91	2.82	2.75	8.45–7.97	6.79
	T$_6$	-	-	9.53	-	-	-	10.426	9.26	2.82	2.70	8.50–7.99	6.70

Pri, pyrimidone ring; Het, heterocyclic ring.

vibration was seen experimentally at 706 cm^{-1} only for compound **4c**. The C—S—C stretching vibrations were theoretically calculated as 663 and 655 cm^{-1} for **4b** and

**Scheme 1.** Synthesis of compound **3**. [Color figure can be viewed at wileyonlinelibrary.com]
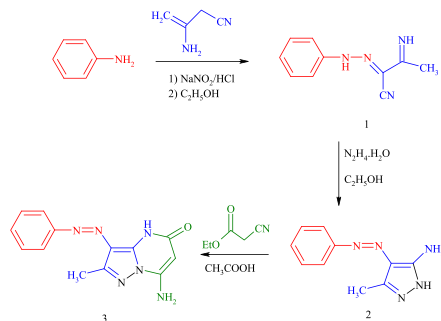
4c, respectively. Finally, C—O stretching vibrations were observed experimentally and theoretically at 1070 and 1078 cm^{-1}, respectively. Theoretical calculations are consistent with experimental results. These results depicted in Table 5. The experimental and theoretical FTIR results show that the dyes **4(a–d)** prefer iminodiazo-enol form (T$_6$), and these results support our previous work [33].

^{1}H NMR analysis of the compounds. The ^{1}H NMR data of the compounds obtained in the DMSO-d_6 solvent gave more specific information about the tautomeric structures of the synthesized compounds. According to the results of ^{1}H NMR spectra, the singlet peaks at the range of 2.45–2.63 ppm were resulted from CH$_3$ protons, and the singlet peak at 3.85 ppm was resulted from —OCH$_3$ protons (for compound **4c**). The peaks of aromatic

Scheme 2. The general route of synthesized dyes **4(a–d)**. [Color figure can be viewed at wileyonlinelibrary.com]
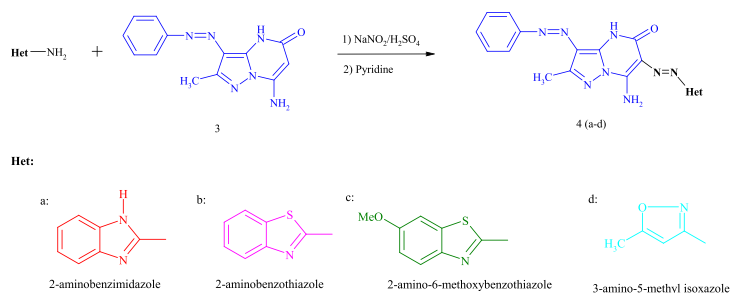
Scheme 3. The tautomeric forms of the compounds.
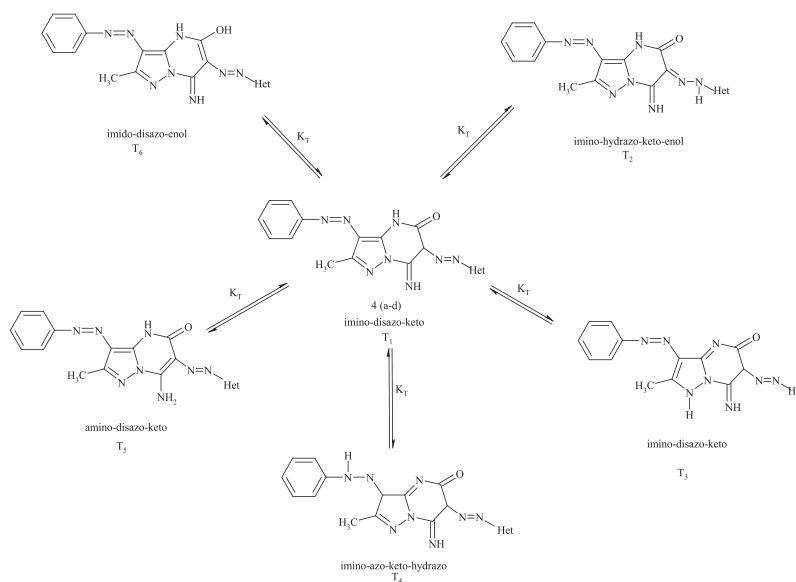
protons were seen at the range of 7.41–8.03 ppm. The broad peaks at the range of 9.87–11.18 ppm were attributed to $=$N$-$H protons and the broad peaks at the range of 10.77–13.02 ppm were attributed to $-$N$-$H protons. O$-$H protons were existed at the range of 12.16–15.98 ppm (Table 6).

As a result of the analysis, we think that this solid compound is present only in imino-diazo-enol form (T_6) for all the dyes due to the OH stretching vibration band presence in the FTIR spectrum, while the observation of the NH stretching vibrations and $=$NH stretching vibrations, absence of C$=$O band, also confirms this idea.

The structural illustration of the tautomers of the compounds is given in Figure 6, and the ^{1}H NMR data, calculated in the DMSO solvent, of the possible tautomeric structures of the compounds are given in Table 7. The Pearson correlation coefficient between the experimental proton NMR of the compounds and the theoretical data of tautomer T_6 was calculated as, on average, $R = 0.95$. The experimental and theoretical ^{1}H NMR results show that the dyes **4(a–d)** prefer iminodiazo-enol form (T_6) and these results also support previous work [33].

CONCLUSION

To summarize the study briefly, four new heterocyclic azo dyes-derived [1,5-*a*] pyrimidine-5-one were successfully synthesized, and their structural characterization was illuminated by FTIR and ^{1}H NMR spectroscopy. The solvatochromic properties of the compounds in different solvents were also studied, and even the change of absorption was determined by the

addition of acid and base to the solution in methanol. While the carbocyclic derivatives of the dyes in previous study did not show positive halochromism, their heterocyclic derivatives in this study showed positive halochromism. The results of the analysis were theoretically examined by the DFT using b3lyp/cc-pvtz method, and the theoretical and experimental results were also compared.

The relationship between six predicted tautomeric structures and electronic properties of compounds was theoretically investigated. The shoulder-free peaks in the experimental UV spectra revealed a single tautomeric form. Six different tautomeric structures were predicted for each of the compounds. As a result of calculations, it was observed that the tautomeric form T_6 having the lowest electronegativity was most suitable with experimental results. Moreover, experimental FTIR and ^{1}H NMR data also showed that tautomer T_6 (iminodiazo-enol form) dominates. It was seen that ^{1}H NMR spectroscopic results of previous study and this study were compatible with each other and were enol tautomeric forms. According to the FT-IR spectroscopic results, the solid forms of some dyes in previous study were keto tautomeric forms, it was observed that the solid forms of dyes in this study enol tautomeric forms. Findings from the calculations show that it is in the relationship between low electronegativity and tautomerism.

EXPERIMENTAL

The reagents and solvents (spectroscopic grade) were purchased from Aldrich (St. Louis, MO) and the Merck Company (Darmstadt, Germany). Melting points of the

dyes were determined using Stuart SMP 30 melting point apparatus (UK). ^{1}H NMR spectra were recorded on a Bruker (Germany) Ultra Shield Plus 400 Mhz spectrometer at room temperature in deuterated dimethyl sulfoxide (DMSO-d_6). Chemical shifts were (Δ) given in ppm. FTIR spectra were recorded on Bruker (Germany) FTIR spectrometer. UV–Vis absorption spectra were recorded on a Shimadzu (Japan) UV-1601 UV–Vis spectrophotometer overt the λ range of 300 to 700 nm. The wavelengths maxima (λ_{max}) were measured in six different solvents such as DMSO, DMF, acetonitrile, methanol, acetic acid, and chloroform at various concentrations (1×10^{-8} to 1×10^{-6} M). Also, shifts of absorption maxima were determined by adding separately 0.1 mL of base (potassium hydroxide, 0.1 M), and 0.1 mL of acid (hydrochloric acid, 0.1 M) in 1 mL of the dye solution in methanol.

Synthesis. Compounds **1**, **2**, and **3** were synthesized according to the literature [33,35,36], respectively. Reaction route is shown in Scheme 1.

General procedure for the synthesis of azo dyes 4(a–d).
Synthesis of 7-amino-6-(1H-indol-2-yl-azo)-2-methyl-3-phenylazo-4H-pyrazolo[1,5-a]pyrimidine-5-one (4a).
Nitrosylsulphuric acid was prepared by dissolving sodium nitrite (0.1 g) in concentrated H_2SO_4 (2 mL) at 70°C. 2-Aminobenzimidazole 0.149 g (1.119 mmol) was dissolved in glacial acetic acid (2.5 mL) and rapidly cooled in an ice-salt bath to 0–5°C. The solution was then added to nitrosylsulphuric acid and the mixture stirred for a further 2 h at this temperature. The resulting diazonium solution was then added in portion over 30 min to a vigorously stirred solution of 7-amino-3-phenylazo-2-methyl-4H-pyrazolo[1,5-a]pyrimidine-5-one (0.3 g, 1.119 mmol), which was dissolved in pyridine (10 mL). The solution was stirred at 0–5°C for 2 h, and the pH of the reaction mixture was maintained at the range of 6–7 by adding sodium acetate solution. The final product separated upon dilution with pure water (50 mL) was filtered, washed with water several times, and dried. It was crystallized with DMSO : water (2:3 by volume) to give 7-amino-6-(1H-indol-2-ylazo)-2-methyl-3-phenylazo-4H-pyrazolo[1,5-a]pyrimidinea-5-one (**4a**) as a light brown solid, yield (67%), mp: decomp < 220°C; FTIR (cm^{-1}) v_{max}: FTIR (cm^{-1}) v_{max}: 3356 (OH), 3198 (NH), 3172 (NH$_{benzimidazole}$), 3065 (=NH), 3065 (Ar—H), 2974 (Aliphatic C—H), 1557 (C=N), 1521 (N=N); ^{1}H NMR (400 MHz, DMSO-d_6) Δ (ppm): 2.62 (3H, s, —CH$_3$), 7.41–7.96 (10H, aromatic), 11.18 (1H, b, pyrimido =NH), 13.02 (1H, b, pyrimido —NH), 15.98 (1H, s, —OH).

The other compounds (**4b–d**) were obtained the same way with the previous procedure. The general synthesis of dyes is illustrated in Scheme 2.

Synthesis of 7-amino-6-(benzothiazole-2-yl-azo)-2-methyl-3-phenylazo-4H-pyrazolo[1,5-a]pyrimidine-5-one (4b). Dark brown solid (72%), decomp > 240°C; FTIR (cm^{-1}) v_{max}:

3231 (OH), 3170 (NH), 3140 (=NH), 3059 (Ar—H), 2951 (Aliphatic C—H), 1609 (C=N), 1548 (N=N), 710 (C—S—C); ^{1}H NMR (400 MHz, DMSO-d_6) Δ (ppm): 2.63 (3H, s, —CH$_3$), 7.41–7.95 (9H, aromatic), 11.12 (1H, b, pyrimido =NH), 12.02 (1H, b, pyrimido —NH), 13.00 (1H, b, —OH).

Synthesis of 7-amino-6-(6-methoxybenzothiazole-2-yl-azo)-2-methyl-3-phenylazo-4H-pyrazolo[1,5-a]pyrimidine-5-one (4c).
Red-brown solid (78%), decomp > 268°C; FTIR (cm^{-1}) v_{max}: 3334 (OH), 3237 (NH), 3212 (=NH), 3064 (Ar—H), 2991 (Aliphatic C—H), 2924 (Aliphatic C—H), 1589 (C=N), 1555 (N=N), 706 (C—S—C); ^{1}H NMR (400 MHz, DMSO-d_6) Δ (ppm): 2.59 (3H, s, —CH$_3$), 3.85 (3H, s, —OCH$_3$), 6.98–8.03 (8H, aromatic), 10.22 (1H, b, pyrimido =NH), 10.88 (1H, b, pyrimido —NH), 12.23 (1H, b, —OH).

Synthesis of 7-amino-6-(5-methylisoxazole-2-yl-azo)-2-methyl-3-phenylazo-4H-pyrazolo[1,5-a]pyrimidine-5-one (4d). Dark green solid (67%), mp: decomp > 284°C; FTIR (cm^{-1}) v_{max}: 3465 (OH), 3235 (NH), 3198 (=NH), 3066 (Ar—H), 2925 (Aliphatic C—H), 1583 (C=N), 1528 (N=N); ^{1}H NMR (400 MHz, DMSO-d_6) Δ (ppm): 2.45 (3H, s, pyrazole —CH$_3$), 2.60 (3H, s, isoxazole —CH$_3$), 6.46–8.01 (6H, aromatic), 9.87 (1H, b, pyrimido =NH), 10.77 (1H, b, pyrimido —NH), 12.16 (1H, b, —OH).

Possible tautomeric structures of the synthesized compounds. Compound **4(a–d)** has six different possible tautomeric forms. As shown in Scheme 3, the forms are imino-diazo-keto (T$_1$), imino-hydrazo-keto-azo (T$_2$), imino-diazo-keto (T$_3$), imino-azo-keto-hydrazo (T$_4$), amino-diazo-keto (T$_5$), and imino-diazo-enol (T$_6$). The possible tautomeric structures were also analyzed theoretically.

Computational details. Kohn-Sham DFT [37,38] was used in the quantum-chemical calculations, and no geometric constraints were made in the optimization processes. The compounds were optimized by using Becke3-Lee-Yang-Parr hybrid exchange-correlation functional (B3LYP) [39,40] with cc-pvtz basis set. Furthermore, mentioned methods were used to obtain UV–Vis, FTIR, and ^{1}H NMR spectra of the compounds. Time-dependent DFT were employed to calculate vertical excitation energies. The self-consistent reaction field method and the conductor-polarizable continuum model were used for UV spectral analysis, in the acetic acid, acetonitrile, DMF, DMSO, chloroform, and methanol phases. Resultant-optimized geometries were used as inputs for vibrational frequencies calculations carried out in gas phase according to the experiments. It was also shown by IR calculations that compounds do not have imaginary frequencies corresponding to local minima on potential energy surfaces. Moreover, ^{1}H NMR calculations of the tautomer structures were carried out in DMSO phase using the same method and basis set.

The HOMO and LUMO energies of both keto forms and tautomeric structures were also calculated with the titled method and basis set. FMO energy eigenvalues of the compounds and their tautomers were used to calculate electronic parameters such as energy band gab ΔE, chemical hardness (η), and electronegativity (χ). The correlation between tautomer structures and electronic parameters of the compounds was investigated. All calculations were performed by using the GAUSSIAN 09 [41] software package program.

REFERENCES AND NOTES

[1] Rawat, A. D.; Sharma, R. S.; Karmakar, S.; Arora, L. S.; Mishra, V. Ecotoxicol Environ Saf 2018, 148, 528.

[2] Özkınalı, S.; Çavuş, M. S.; Sakin, B. JOTCSA, Section A: Chemistry 2018, 5, 159.

[3] Rotaru, A.; Dumitru, M. J Therm Anal Calorim 2017, 127, 21.

[4] Bakan, E.; Karci, F.; Avinç, O. Int J Eng Appl Sci 2016, 10, 8269.

[5] Kocaokutgen, H.; Gür, M.; Soylu, M. S. Lönnecke Acta Crystallogr E 2003, E59, 1613.

[6] Geng, J.; Xu, D.; Chang, F.; Tao, T.; Huang, W. Dyes and Pigments 2017, 137, 101.

[7] Akiyama, H.; Kawara, T.; Takada, H.; Takatsu, H.; Chigrinov, V.; Prudnikova, E.; Kozenkov, V.; Kwok, H. Liq Cryst 2002, 29, 1321.

[8] Ledoux, I.; Zyss, J.; Barni, E.; Barolo, C.; Diulgheroff, N.; Quagliotto, P.; Viscardi, G. Synth Met 2000, 115, 1 213.

[9] Aliabadi, A.; Eghbalian, E.; Kiani, A. Iran J. Basic Med Sci 2013, 16, 1133.

[10] Zayed, M. A.; Mohamed, G. G.; Abdullah, S. A. M. Spectrochim Acta A 2011, 78, 1027.

[11] Kumar, K.; Chinnagiri, T.; Keshavayya, J.; Rajesh, T. N.; Peethambar, S. K.; Ali, S.; Angadi, R. Org Chem Int 2013, 2013, 1.

[12] Maradiya, H. R. JSerbChemSoc 2002, 67, 709.

[13] Otutu, J. O. IJRRAS 2013, 15, 292.

[14] Castro, M. C. R.; Schellenberg, P.; Belsley, M.; Fonseca, A. M. C.; Fernandes, S. S. M.; Raposo, M. M. M. Dyes and Pigments 2012, 95, 392.

[15] Hallas, G.; Choi, J. H. Dyes and Pigments 1999, 42, 249.

[16] Hallas, G.; Towns, A. D. A. Dyes and Pigments 1996, 31, 273.

[17] Xu, D.; Li, Z.; Peng, Y.; Geng, J.; Qian, H.; Huang, W. Dyes and Pigments 2016, 133, 143.

[18] Abdou, M. M. Am J Chem 2013, 3, 126.

[19] Ünal, A.; Eren, B.; Eren, E. J Mol Struct 2013, 1049, 303.

[20] Dostanic, J.; Mijin, D.; Uscumlic, G.; Jovanovic, D. M.; Zlatar, M.; Loncarevic, D. Spectro Chim Acta Part A 2014, 123, 37.

[21] Özkinali, S.; Çavuş, M. S.; Ceylan, A.; Gür, M. J Mol Struct 2017, 1149, 206.

[22] Tsai, P. C.; Wang, J. Dyes and Pigments 2008, 76, 575.

[23] Hassan, A. S.; Mady, M. F.; Awad, H. M.; Hafes, T. S. Chinese Chem Lett 2017, 28, 388.

[24] Laikhter, A.; Behlke, M. A.; Walder, J.; Roberts, K. W. US Patent No 9,540,515.10 Jan. 2017.

[25] Karcı, F.; Sener, N.; Yamaç, M.; Sener, I.; Demirçalı, A. Dyes and Pigments 2009, 80, 47.

[26] Kees, K. L.; Fitzgerald, J. J.; Steiner, K. E.; Mattes, J. F.; Mihan, B.; Tosi, T.; Mondoro, D.; McCaleb, M. L. J Med Chem 1996, 39, 3920.

[27] Kelekçi, N. G.; Yabanoğlu, S.; Küpeli, E.; Salgın, U.; Özgen, Ö.; Uçar, G.; Yesilada, E.; Kendi, E.; Yesilada, A.; Bilgin, A. A. Bioorgan Med Chem 2007, 15, 5775.

[28] Faidallah, H. M.; Rostom, S. A. F. Arch Pharm 2017, 350, e1700025.

[29] Malvar, D. C.; Ferreira, R. T.; Castro, R. A.; Castro, L. L.; Freitas, A. C. C.; Costa, E. A.; Florentino, I. F.; Mafra, J. C. M.; Souza, G. E. P.; Vanderlinde, F. A. Life Sci 2014, 95, 81.

[30] Shehry, M. F. E.; Ghorab, M. M.; Abbas, S. Y.; Fayed, E. A.; Shedid, S. A.; Ammar, Y. A. Eur J Med Chem 2018, 143, 1463.

[31] Hernández-Vázquez, E.; Aguayo-Ortiz, R.; Ramírez-Espinosa, J. J.; Estrada-Soto, S.; Hernández-Luis, F. Eur J Med Chem 2013, 69, 10.

[32] Soliman, R.; Mokhtar, H.; Mohamed, H. F. J Pharm Sci 1983, 72, 1004.

[33] Şener, N.; Erişkin, S.; Yavuz, S.; Şener, İ. J Heterocyclic Chem 2017, 54, 3538.

[34] Ma, M.; Johnson, K. E. J Electroanal Chem 1993, 355, 97.

[35] Elnagdi, M. H.; Sallam, M. M. M.; Fahmy, H. M.; Ibrahim, S. A. M. Helv Chim Acta 1976, 59, 551.

[36] Elnagdi, M. H.; Elgemeie, G. E.; Abd-Elaal, F.-M. Heterocycles 1985, 23, 3121.

[37] Hohenberg, P.; Kohn, W. Phys Rev 1964, 136, B864.

[38] Kohn, W.; Sham, L. Phys. Rev. 1965, 140, A1133.

[39] Becke, A. D. J Chem Phys 1993, 98, 1372.

[40] Lee, C.; Yang, W.; Parr, R. G. Phys Rev, B 1988, 37, 785.

[41] Frisch, M. J.; Trucks, G. W.; Schlegel, H. B.; Scuseria, G. E.; Robb, M. A.; Cheeseman, J. R.; Scalmani, G.; Barone, V.; Mennucci, B.; Petersson, G. A.; Nakatsuji, H.; Caricato, M.; Li, X.; Hratchian, H. P.; Izmaylov, A. F.; Bloino, J.; Zheng, G.; Sonnenberg, J. L.; Hada, M.; Ehara, M.; Toyota, K.; Fukuda, R.; Hasegawa, J.; Ishida, M.; Nakajima, T.; Honda, Y.; Kitao, O.; Nakai, H.; Vreven, T.; Montgomery, J. A.; Peralta, J. E.; Ogliaro, F.; Bearpark, M.; Heyd, J. J.; Brothers, E.; Kudin, K. N.; Staroverov, V. N.; Keith, T.; Kobayashi, R.; Normand, J.; Raghavachari, K.; Rendell, A.; Burant, J. C.; Iyengar, S. S.; Tomasi, J.; Cossi, M.; Rega, N.; Millam, J. M.; Klene, M.; Knox, J. E.; Cross, J. B.; Bakken, V.; Adamo, C.; Jaramillo, J.; Gomperts, R.; Stratmann, R. E.; Yazyev, O.; Austin, A. J.; Cammi, R.; Pomelli, C.; Ochterski, J. W.; Martin, R. L.; Morokuma, K.; Zakrzewski, V. G.; Voth, G. A.; Salvador, P.; Dannenberg, J. J.; Dapprich, S.; Daniels, A. D.; Farkas, O.; Foresman, J. B.; Ortiz, J. V.; Cioslowski, J.; Fox, D. J. Gaussian 09, Revision B.01; Gaussian, Inc: Wallingford CT, 2010.

SUPPORTING INFORMATION

Additional supporting information may be found online in the Supporting Information section at the end of the article.